Electronic Supplementary Material (ESI) for Dalton Transactions.
This journal is © The Royal Society of Chemistry 2016

Supporting Information

Role of the metal cation types around VO_4 groups on the nonlinear optical behavior of materials: experimental and theoretical analysis

Xin Su,[ab] Zhihua Yang,*[a] Guopeng Han,[ab] Ying Wang,[a] Ming Wen,[ab] Shilie Pan*[a]

[a] Key Laboratory of Functional Materials and Devices for Special Environments of CAS; Xinjiang Key Laboratory of Electronic Information Materials and Devices, Xinjiang Technical Institute of Physics & Chemistry of CAS, 40-1 South Beijing Road, Urumqi 830011, China;

[b] University of Chinese Academy of Sciences, Beijing 100049, China;

Corresponding Author

To whom correspondence should be addressed. Phone: (86)991-3810816

Fax: (86)991-3838957. E-mail: zhyang@ms.xjb.ac.cn (Zhihua Yang).

slpan@ms.xjb.ac.cn (Shilie Pan)

Experimental Details

Synthesis

Reagents: K_2CO_3 (99.0%), CdO (99.5%), V_2O_5 (99.0%) were used as received. Polycrystalline samples of $KCd_4(VO_4)_3$ were prepared by standard solid state reaction. Stoichiometric proportions of raw materials were mixed and presintered at 500 °C for 10 h. Then the mixtures were elevated to sintering temperatures of 780 °C and hold at this temperature for one week with several intermittent grindings. The powder samples were characterized bypowder X-ray diffraction.

Powder X-ray Diffraction (PXRD)

PXRD patterns of polycrystalline samples were obtained on a Bruker D2 PHASER diffractometer with Cu Kradiation (λ = 1.5418 Å) at room temperature. The 2θ range was 10–70° with a step size of 0.02° and a fixed counting time of 1s per step. The PXRD pattern of the bulk polycrystalline phase of $KCd_4(VO_4)_3$ is in good agreement with the calculated pattern derived from the single-crystal data and is shown in Fig.S2a.

UV-vis-NIR Diffuse Reflectance Spectra

UV-vis-NIR diffuse reflectance spectra (Fig.S2b) were recorded on a Shimadzu Solid Spec-3700DUV spectrophotometer at room temperature. Data were collected in the wavelength range of 190 to 2500 nm. Therefore, $KCd_4(VO_4)_3$ possesses a wide transmittance range from visible (vis) to near-infrared (NIR) regions, also indicates that the band gap of $KCd_4(VO_4)_3$ is 2.75 eV.

ComputationalDetails

The experimental X-ray crystallographic data of $KCd_4(VO_4)_3$ and $Ca_3(VO_4)_2$ were used as the initial geometry for the theoretical calculations. The first-principles calculations are performed by the plane-wave pseudo-potential method[1-3] which employs a local basis set implemented in the CASTEP package[4] based on the DFT. The exchange correlation interaction was treated by the LDA with the Ceperley and Alder-Perdew-Zunger functional (CA-PZ). The ion-electron interactions were modeled by the optimized normal-conserving pseudo-potential (NCP) for all elements,[5, 6] the valence electrons were treated with a plane wave basis set, and the core electrons were handled by pseudo-potential approximations.[5,7, 8]

For the purpose of achieving energy convergence, a plane-wave basis set energycutoff was 750 eV, and the Monkhorst-Pack[9] scheme was given by 3× 3 × 6 inthe irreducible Brillouin zone(BZ).[10] The optimized electronic configurations of the ground state atoms form for K$3s^2 3p^6 4s^1$, Cd $4d^{10}5s^2$, Ca$3s^2 3p^6 4s^2$,V $3d^3 4s^2$, and O $2s^2 2p^4$, within the primitive cell along the *c* direction. Our convergence tests reveal that the above computational parameters are sufficiently accurate for present purposes.

Band Structure and Density of States of $KCd_4(VO_4)_3$and $Ca_3(VO_4)_2$

In view of the forthcoming calculations of the electronic band structure and density of states, it is necessary to perform an optimization of the initial crystal structure (Fig.S3 and Fig.S4). To investigate the relationship between microscopic and macroscopic properties, population analyses based on the electronic structures were obtained for $KCd_4(VO_4)_3$ and $Ca_3(VO_4)_2$.

The calculated energy bands along the line of high symmetry points in the BZ are illustrated in Fig.S4a and S5a. The total density of states (DOS) and partial densities of states (PDOS) projected on the constituent atoms in $KCd_4(VO_4)_3$ and $Ca_3(VO_4)_2$ crystal are shown in Fig.S3b and S4b, which focuses on the electronic states close to the energy band gap. For $KCd_4(VO_4)_3$ and $Ca_3(VO_4)_2$, there are found that an indirect LDA band gap of 2.58eV and 3.63 eV expands from the valence band (VB)maximum located at Γ point and the conduction band (CB)minimum located at Z point, respectively (Fig.S7).The Mulliken population analysis is displayed in Table S1 and Table S2. The calculated result reveals that the V–O bonds show more covalent character than other bonds (Table S2). The calculated Mulliken charge population of $KCd_4(VO_4)_3$ and $Ca_3(VO_4)_2$, the K-O, Cd-O, Ca-O and V-O bonds are 1.23, 1.09 ~ 1.17, 1.31~ 1.39 and 0.59 ~ 0.79e (charge unit), respectively. It is obvious that the overlap populations have the following orders: $(VO_4)^{3-}$>$(CdO_4)^{6-}$. The calculated bond orders of K-O, Cd-O, Ca-O and V-O bonds(in $KCd_4(VO_4)_3$ and $Ca_3(VO_4)_2$) are 0~ 0.02, 0.16 ~ 0.27,-0.03 ~ 0.07 and 0.59-0.83 e, respectively (Table S5). Accordingly, we can say that the covalent character of the V-O bonds is slightly larger than that of the Cd-O bonds (covalent single-bond order is generally1.0e).

We are aslo able to identify the origin of the various orbits from the PDOS to $KCd_4(VO_4)_3$ and $Ca_3(VO_4)_2$. Here we just give the detail for $KCd_4(VO_4)_3$, we clearly see that the highest occupiedand lowest unoccupied state levels respectively come from non-bonding O-2*p* from Fermi Level (FL) to about -0.12 eV and V orbits local at the CB minimum as shown in Figures S6. The energy range from -0.12 to -5.0 eV in VB region has significant contributions from O-*p* mixing with V-*d* and Cd-*p* states. In the energy region from -6.0 eV to -8.0 eV, however, the contributions of Cd-*d*, Cd-*p* and K-*p* are apparent in addition to O-2*p* states. As for CBs, the bands above the FL aremainly derived from V-3*d*, O-2*p*, Cd-*p* states with slight contribution of *s* and *p* orbitals of K. This could be a major reason why $KCd_4(VO_4)_3$ has a narrower band gap compared with LVO, $KCd_4(VO_4)_3$ and $Ca_3(VO_4)_2$ crystals.

References

(1) Aversa, C.; Sipe, J. E. *Phys. Rev. B*1995, **52**, 14636.

(2)Janak, J. F. *Phys. Rev. B* 1978,**18**,7165.

(3) Payne, M. C.; Teter, M. P.; Allan, D. C.; Arias, T. A.; Joannopoulos, J. D. *Rev. Mod.Phys.*1992, **64**, 1045.

(4) Clark, S. J.; Segall, M. D.; Pickard, C. J.; Hasnip, P.J.; Probert, M.J.; Refson, K.; Payne, M.C.*Z. Kristallogr.*2005, 220, 567.

(5) Kohn, W.; Sham, L. J. *Phys. Rev.* 1965,**140**, 1133.

(6) Perdew, J. P.; Burke, K.; Ernzerhof, M.*Phys. Rev. Lett.* 1996,**77**,3865.

(7) Anisimov, V.I.; Aryasetiawan, F.; Lichtenstein, A.I.*J. Phys*:*Condensed Matter.*1997,**9**, 767.

(8) Lin, J. S.; Qteish, A., Payne, M. C.; Heine, V. *Phys. Rev. B*1993,**47**, 4174.

(9) Monkhorst, H. J.; Pack, J. D. *Phys. Rev.B*1976,**13**,5188.

(10) Perdew, J. P.; Wang, Y. *Phys. Rev. B*1992, **45**, 13244.

TableS1. Mulliken charge population of $KCd_4(VO_4)_3$ and $Ca_3(VO_4)_2$.

(a)$KCd_4(VO_4)_3$

Atom	K	Cd	V	O
Population	1.23	1.09 ~1.17	0.78 ~ 0.79	-0.59~- 0.72

(b)$Ca_3(VO_4)_2$

Atom	Ca	V	O
Population	1.31~ 1.39	1.03	-0.69~ -0.79

TableS2. Bond distances *d* and Mulliken overlap populations Q(|*e* |)for characteristic atomic pairs in $KCd_4(VO_4)_3$ and $Ca_3(VO_4)_2$

(a)$KCd_4(VO_4)_3$

Value Atomic pair	bond distances *d* (Å)	overlap populations
K-O	2.6163(1) ~ 2.9426(8)	0~ 0.02
Cd-O	2.1647(9) ~2.8436(3)	0.16 ~ 0.27
V-O	1.5667(8) ~ 1.6604(2)	0.59~ 0.76

(b)$Ca_3(VO_4)_2$

Value Atomic pair	bond distances *d* (Å)	overlap populations
Ca-O	2.6814(6) ~ 2.3930(3)	-0.03 ~ 0.07
V-O	1.6369(4) ~ 1.8219(9)	0.73~ 0.83

Figure S1. The phase diagram of $LiVO_3$-Li_3VO_4 system (The transition above 750◦C to the γ_{II} phase via an intermediate phase has no counterpart among the β and γ phases. The temperature phase is an orthorhombic phase which is very similar to both β and γ phases Li_3VO_4).

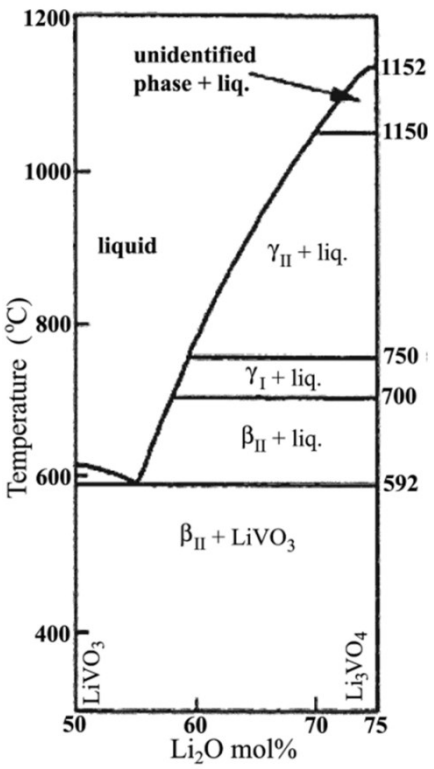

Figure S2. The metal cation coordination around the VO_4 groups in β_{II}-Li_3VO_4(a), $KCd_4(VO_4)_3$(b) and $Ca_3(VO_4)_2$(c) crystals, respectively.

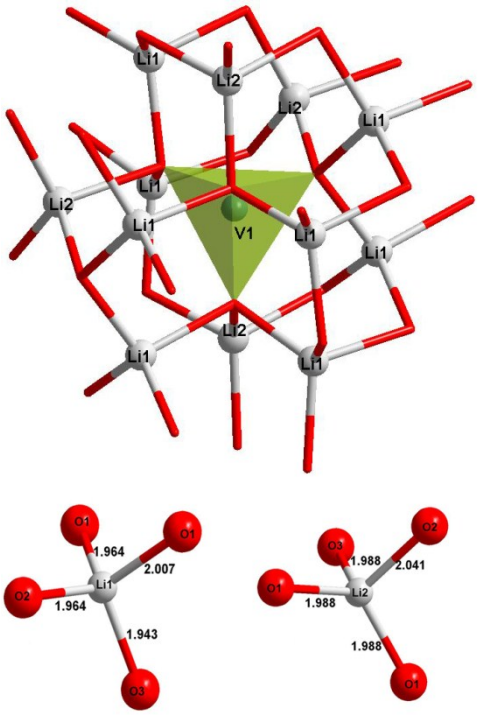

(a)

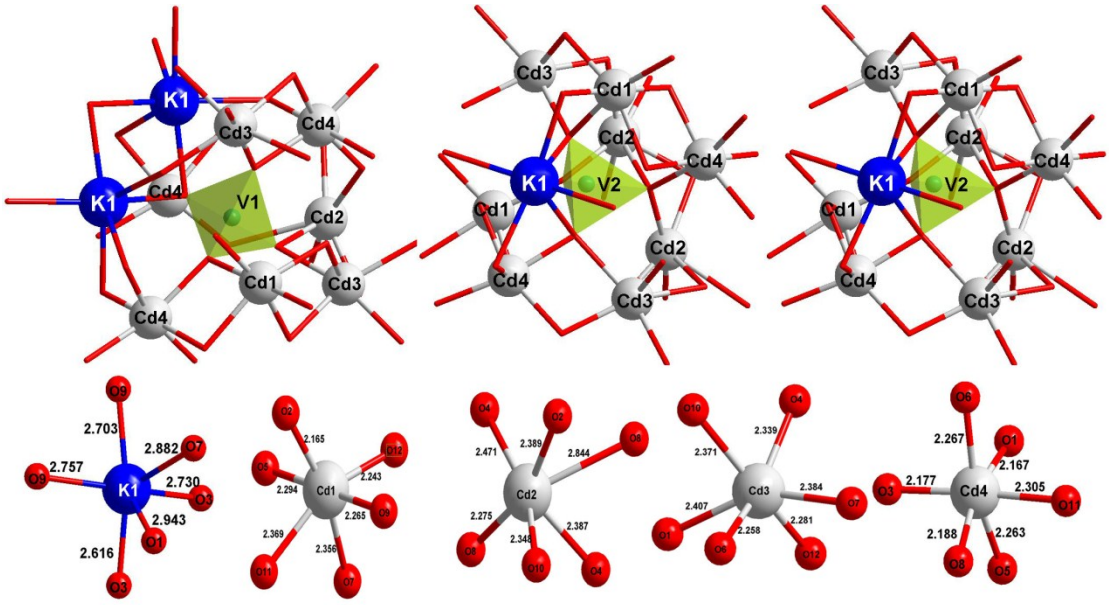

(b)

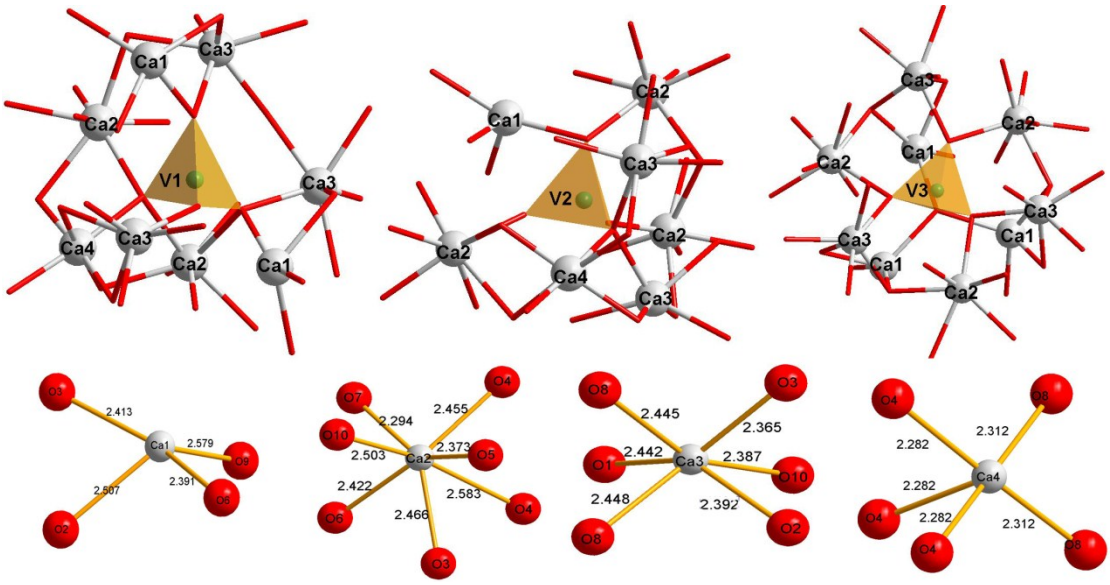
Ca1
Ca3
Ca2
V1
Ca3
Ca4
Ca3
Ca2
Ca1
Ca2
Ca1
Ca3
V2
Ca2
Ca2
Ca4
Ca3
Ca3
Ca2
Ca1
V3
Ca3
Ca3
Ca1
Ca1
Ca2
O3
2.413
Ca1
2.579
O9
2.391
O6
2.507
O2
O7
2.294
2.455
O4
O10
2.503
Ca2
2.373
O5
2.422
2.583
O4
O6
2.466
O3
O8
2.445
O3
2.365
O1
2.442
Ca3
2.387
O10
2.448
2.392
O8
O2
O4
O8
2.282
2.312
Ca4
2.282
O4
2.282
2.312
O4
O8

(c)

Figure S3. (a) Experimental and calculated XRD patterns for $KCd_4(VO_4)_3$. (b) UV−vis diffuse reflectance spectrum for $KCd_4(VO_4)_3$.

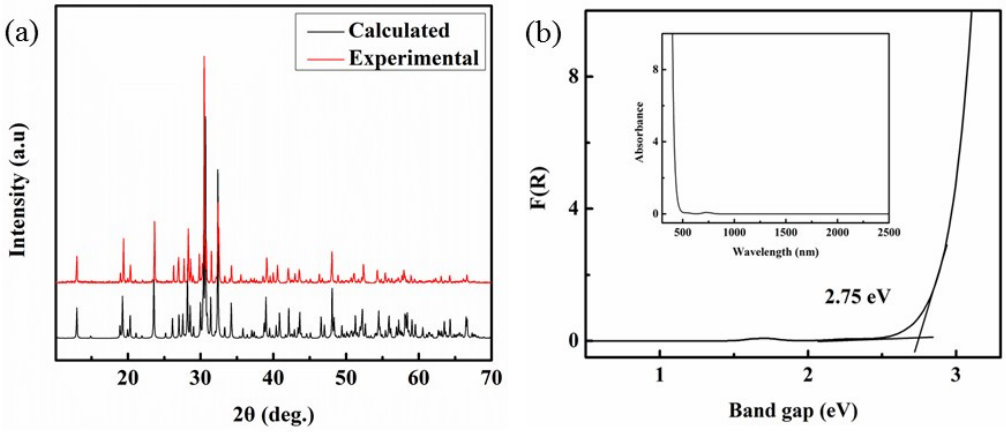

Figure S4. Band structure(a) and DOS(b) of $KCd_4(VO_4)_3$.

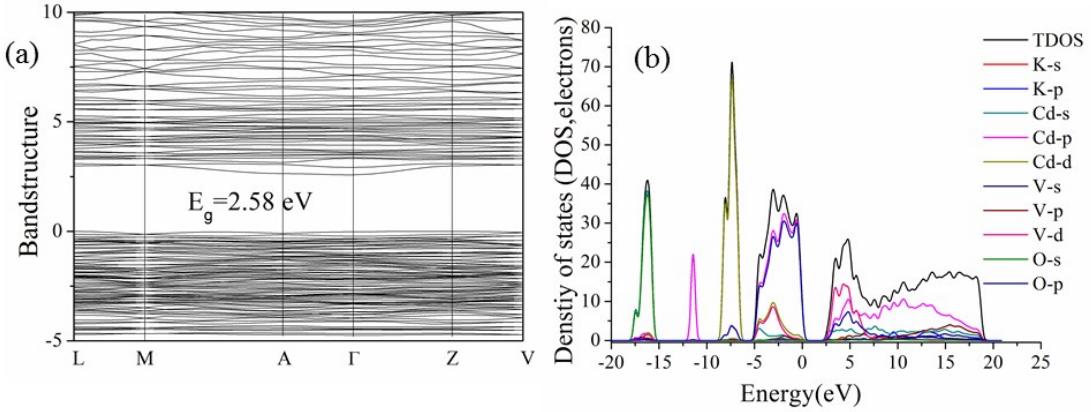

Figure S5. Band structure(a) and DOS(b) of $Ca_3(VO_4)_2$.

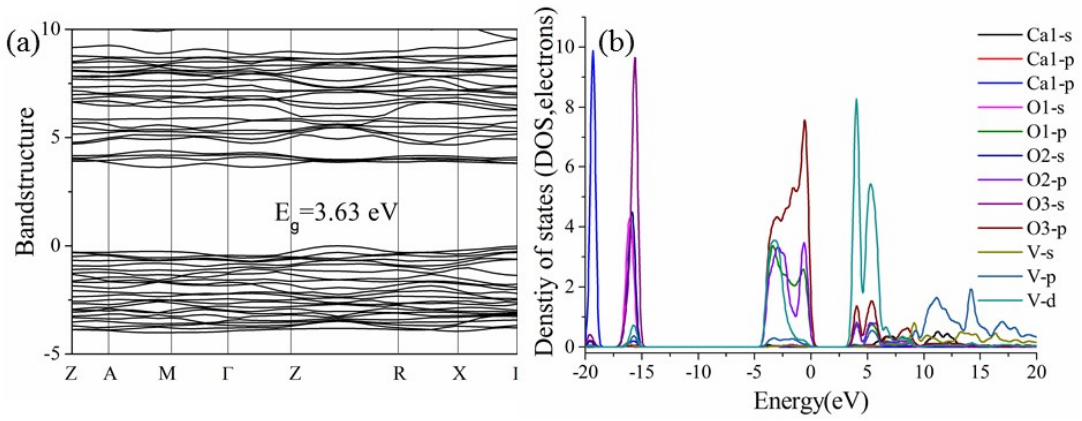

Figure S6. Proposed atom-orbital bonding diagram for VO_4 in Li_3VO_4.((a) atomic level, (b) crystal-field split level, and(c) final interaction states. The solid and dashed lines represent largeand small contributions, respectively.)

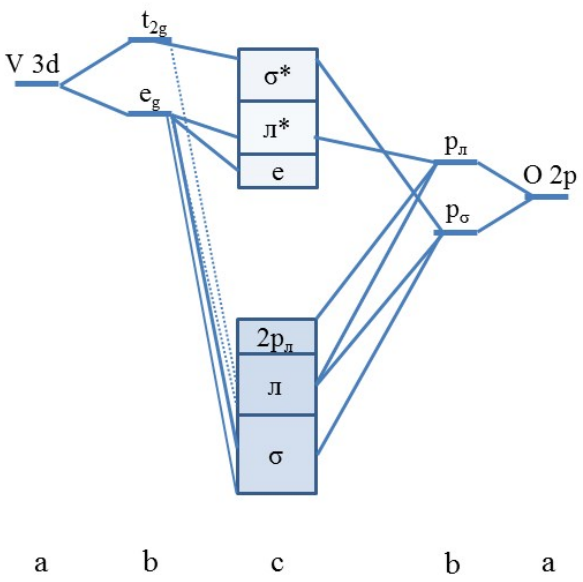
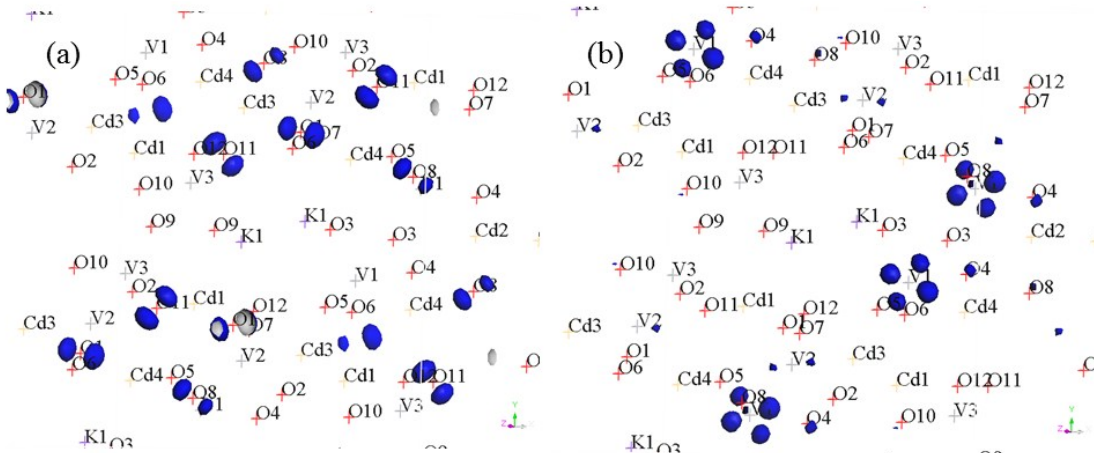
Figure S7.The energy range of the specific orbitals (the highest occupied orbitalsand lowest unoccupied orbitals) of the $KCd_4(VO_4)_3$ crystals shown in (a) (b).